International Journal of Mass Spectrometry 298 (2010) 55–63

Contents lists available at ScienceDirect

International Journal of Mass Spectrometry

journal homepage: www.elsevier.com/locate/ijms

Generation of current pulses in collector electrode of IMS detectors

Jarosław Puton [a,*], Bogusław Siodłowski [b]

[a] Laboratory of Applied Environmental Chemistry, Department of Environmental Sciences, University of Kuopio, Patteristonkatu 1, FI-50100 Mikkeli, Finland
[b] Institute of Chemistry, Faculty of Advanced Technologies and Chemistry, Military University of Technology, ul. Kaliskiego 2, 00-908 Warsaw, Poland

ARTICLE INFO

Article history:
Received 24 December 2008
Received in revised form 1 February 2010
Accepted 3 February 2010
Available online 12 February 2010

Keywords:
Ion mobility spectrometry
Ion movement
Aperture grid

ABSTRACT

Precise investigations of phenomena related to generation of the signal in the collector electrode of ion mobility spectrometer have been conducted. A two-dimensional mathematical model of electric field considering the structure of the aperture grid has been developed. Based on that model static properties of the aperture grid–collector system, i.e., the transmittance of the aperture grid as a function of polarisation potential and shielding efficiency of the grid were estimated. Dynamic effects have also been modeled. For this purpose, a computer simulation of ionic swarm movement and calculation of the electric field generated by elements of that swarm have been applied. The procedure enabled estimation of time dependence of collector current components, and in consequence, determination of a peak shape in the drift time spectrum.

Results of theoretical considerations and calculations have been verified by comparison with experimental data obtained with ion mobility spectrometer prepared for investigation of structural parameters effect on output signal.

1. Introduction

Detectors used in the ion mobility spectrometry (IMS) can be classified as selective ionisation detectors. A classic IMS detector consists of an ion reactor, in which a sample is ionised, and a drift section destined for separation of ions. This technology was developed nearly 40 years ago [1]. Since that time, alternative constructions such as aspiration spectrometers [2] and devices with high electric field [3,4] have been studied and used in commercial instruments. However, due to their advantages, classic IMS detectors are still successfully used in practice. High selectivity is a feature distinguishing those detectors from more modern technical solutions. It depends mainly on the resolving power defined as quotient of drift time and width-at-half-height of the peak in the drift time spectrum. In case of the best detectors the value of this parameter exceeds 100 [5,6], but usually it is lower, e.g., for the IMS detector used for this study the resolving power was about 30.

Width of the peak in the drift time spectrum depends on many factors. Spangler and Collins [7] analysed the most important phenomena affecting the shape of the peak. In their model, the shape of ion concentration distribution in the beginning of the drift section is rectangular. Finite width of that distribution is the main instrumental factor affecting the peak shape. The most significant physical mechanism responsible for peak broadening is diffusion occurring during movement of ions along the drift section. The Spangler and Collins' model allows effective optimisation of the drift section length and value of electric field, in which drift of ions takes place. Apart from diffusion, broadening of ion swarm may be caused by a phenomenon of mutual repulsion, defined also as a space charge effect [8]. That effect is noticeable when charge density in an ion cloud is high. A significant effect of that phenomenon on resolving power was observed for the IMS detector in which laser ionisation was used [9].

More precise analysis of phenomena occurring in IMS detectors shows that the peak shape in the drift time spectrum depends on the details of the drift section structure and the construction of neighbouring elements. Portion of ions is introduced into the drift region through a shutter grid, constituting a kind of electrostatic valve, which separate the ion reactor from the drift space. Electric field in vicinity of the grid is not uniform and is variable in time [10]. If distance between the grid electrodes is comparable with space covered by ions in time equal to gating pulse duration, initial distribution of ion concentration significantly differs from one-dimensional rectangular distribution. Using simple computer simulations it may be shown that ions are introduced to the drift section between grid electrodes in form of numerous swarms separated from each other [11]. Therefore, phenomena taking place in the neighbourhood of the shutter grid constitute an instrumental factor influencing the peak shape at the first phase of the drift. Another often described effect associated with construction of the IMS detector is non-homogeneity of electric field in the drift sec-

* Corresponding author. Tel.: +48 22 683 71 82/608 42 40 40; fax: +48 683 85 82.
E-mail addresses: jputon@wat.edu.pl, jarek.puton@wp.pl (J. Puton).

1387-3806/$ – see front matter © 2010 Elsevier B.V. All rights reserved.
doi:10.1016/j.ijms.2010.02.005

tion [12,13]. It causes diversity of the drift times for ions moving in different distances from the axis of the detector.

An enhanced model of phenomena influencing signal shape from the IMS detectors was presented by Spangler [14]. According to that model, processes occurring in the last passage of the drift path, i.e., in the space between the aperture grid and the collector electrode, play a very important role. Here, two mechanisms of current generation are crucial: electric induction and transfer of ionic charge to the collector. A signal from the detector is already created in the time when ions are able to induce the charge on collector surface. In the Spangler's model [14] electric field produced by ions affects the collector after ions cross the aperture grid. Ionic movement in front of the grid does not influence the value of the collector current. Generation of the current ends when all ions are collected. Therefore, the shape of the peak resulting from the previously mentioned effects depends also on the instrumental factor associated with construction of aperture grid and ion collector.

The main objective of this work is to describe processes of current generation in the collector electrode using a model involving structure of the aperture grid. In reality the grid is not an amorphous plane perfectly shielding the collector but it is made of electrodes having definite dimensions and placed in a determined distance from the collector. Mathematical model of the system involving the aperture grid and the collector, fitted to real geometry, cannot be one-dimensional. In this work a two-dimensional model was applied. The model proved sufficient for correct description of phenomena occurring in the neighbourhood of the ion collector. Unlike one-dimensional models [7,14] in that case it is impossible to perform effective analytical calculations. Therefore, all the presented theoretical results were obtained by the numerical methods.

2. Instrumentation and experimental procedures

Results obtained directly based on the mathematical model of the IMS detector are multidimensional functions describing spatial or surface distributions of values including electric field, ion concentration, or the surface charge density. Unfortunately, experimental verification of that kind of results is very difficult or even impossible to accomplish. In practice the only parameter that can be calculated and measured is the electric current flowing in the circuit of the collector electrode. For that reason quantity of experimental data collected in order to verify the mathematical model is low.

Measurements were carried out for the detector named MedIMS. It was built in Military University of Technology in Warsaw (Poland) in order to investigate effect of the detector's elements structure on operational parameters. Total length of this instrument is equal to about 9.5 cm, length of drift section is 4.7 cm and its diameter is 2.0 cm. As ionisation source 5 mCi ^{63}Ni is applied. The outline of the detector structure with the voltage divider used in measurements is presented in Fig. 1.

Phenomena described in this work take place in vicinity of the collector and for that reason dimensions of elements in that region are of particular importance. The aperture grid is made of 0.10-mm-thick etched beryllium bronze plate. Width of grid electrodes is equal to 0.18 mm and the distance between their centres is 1.00 mm. The grid is separated from the base electrode by 0.5-mm-thick Teflon foil. A distance between the grid and the collector electrode surface is about 1.0 mm.

The IMS detector co-operated with self-built electronic instruments, i.e., electrometric amplifier and pulse generator controlling the shutter grid. An amplifier was constructed on the principle of the current-to-voltage converter. Its gain may be changed in the range from 1.0 to 20 V/nA. Time of the amplifier output signal build-up (0–90%) for stimulus in form of step function is less than

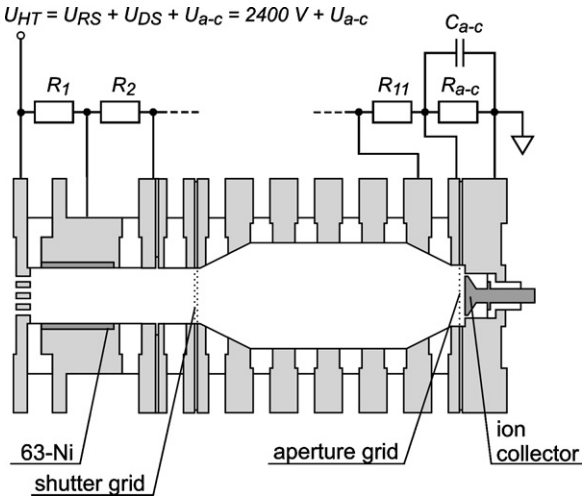

Fig. 1. MedIMS detector—outline of structure with elements of the voltage divider.

10 μs. In measurements of constant current, the output signal from the amplifier was measured with a digital voltmeter, whereas the drift time spectra were registered with the digital scope Yokogawa DL1620S interfaced with a computer. High voltage necessary for polarisation of detectors electrodes was supplied from the power supply ZWN-42 (POLON).

Measurements of constant current and the drift time spectra were made for different values of voltage U_{a-c} between the aperture grid and the ion collector. During the current measurements shutter grid electrodes were shorted what corresponds to "opening" of the grid. Drift time measurements were conducted at gating pulses duration, t_g, equal to 0.2 ms. U_{a-c} voltage was adjusted by exchange of R_{a-c} resistor in the voltage divider (see Fig. 1). For every R_{a-c} resistance, the value of supplying voltage U_{HT} was selected in such a way that the sum of potential drops along the reaction section U_{RS} and the drift section U_{DS} was maintained constant ($U_{RS} + U_{DS} = 2400$ V). Therefore, changes of the electric field in vicinity of the collector did not affect the electric field in other regions of the IMS detector.

The R_{a-c} resistor is shunted with a 100 nF C_{a-c} capacitor. This is a common solution which aim is to reject the effect of parasitic capacity existing between the grid and collector on dynamic properties of current measurement circuit. Existence of the C_{a-c} capacitor does not influence significantly the value of the electric field in vicinity of the collector.

All measurements were carried out at the detector temperature of 80 °C. The air dried with 5 A molecular sieves was flowing through the reaction and drift sections of the detector. The drift gas flow rate was 500 ml/min and carrier gas flow rate was typically 300 ml/min.

3. Modeling of phenomena in vicinity of collector electrode

Description of processes occurring in ionised gases requires calculation of electric field values and distribution of ionic concentration. The first of the these problems leads to solution of Laplace or Poisson's equation, and the second one to solution of transport equation defined for the phenomena taking place in the IMS detectors as, so called, advection–diffusion problem [15]. In case of analysis of phenomena occurring in vicinity of the collector electrode, the solution of the non-stationary problems is essential, because the final goal is to find time dependence of current flowing from the collector. However, some practically significant properties of a system consisting of the collector and the aperture grid can be estimated based on static considerations.

All the electric field distributions presented in this work were determined with Partial Differential Equation Toolbox (PDE-T), included in the MATLAB software package [16]. Matrixes of the electric field potential generated with this software were used for drawing electric field lines, determination of ion swarm location and calculation of the charge induced in the collector. Most of these operations were completed with a computer program IMS-AG created for this purpose in DELPHI 7. Some calculations, e.g., multiple solutions of Poisson equation in order to calculate the function used for determination of surface charge in the collector, were carried out using more sophisticated MATLAB's functions.

3.1. Electric field in the system of detector's electrodes

The IMS detector can be considered as a set of metal electrodes surrounding space, where ions are moving. Electric potentials of particular electrodes are determined by connecting them to the voltage source with a suitable voltage divider. Metal electrodes produce the electric field E_{me} in the space inside the detector. If swarms of ions are present in that space, they become a source of additional field E_{ion}. Total electric field is the sum of those two components:

$$E = E_{me} + E_{ion} \quad (1)$$

In typical constructions the electric field E_{me} produced by metal electrodes of the drift section in the IMS has the value of 200–400 V/cm. It is nearly uniform and directed along the detector axis.

Electric field E_{ion} generated by the charge of ions has different properties than field E_{me}. If we assume that ionic cloud injected through the shutter grid to the drift section of the detector has diameter of 2 cm and thickness of 0.2 cm, then, for ion concentration equal to 10^7 cm^{-3} the maximum intensity of the electric field E_{me} is less than 2 V/cm. That value is much smaller than intensity of the field generated by metal electrodes. Therefore, for analysing phenomena occurring in the drift space, it can be assumed (with good accuracy) that ionic movement occurs under the effect of the field E_{me} only. In more precise analyses of resolving power of the IMS detectors, effect of mutual repulsion related to the field E_{ion} is also considered [8]. Electrostatic repulsion effect was neglected in calculations carried out in this work because of a great difference in intensities of both field components.

The electric field E_{ion} is not homogeneous. If the disc-shaped cloud of the ions is placed far from the collector then the field in vicinity of this electrode has axial symmetry and its intensity strongly depends on the distance between the ionic swarm and the collector. When ions are very close to the collector, i.e., the distance between edge of swarm and collector is much smaller than the diameter of the swarm, the electric field can be calculated using flat, two-dimensional geometry.

The most important feature distinguishing both components of the electric field is that the field E_{me} is constant in time, while the component E_{ion} depends on the position of ionic swarm, so it is variable in time. It causes the induction of variable electric charge on surfaces of electrodes surrounding the moving swarm of ions. This effect occurs also in the collector and results in generation of induced current being a component of the signal from the IMS detector. Problems of signal generation are discussed in details in Section 3.2.

Electric field produced by metal electrodes E_{me} in vicinity of the collector was computed by solving the Laplace's equation for geometry presented in Fig. 2a. Boundary conditions for that problem correspond to the constant value of the electric field far from the grid and to defined potentials of the grid and the collector. Because of symmetry of the problem, zeroing of normal component of the electric field for remaining planes can be assumed. Distribution of the electric potential value φ_{me} depends on dimensions of discussed

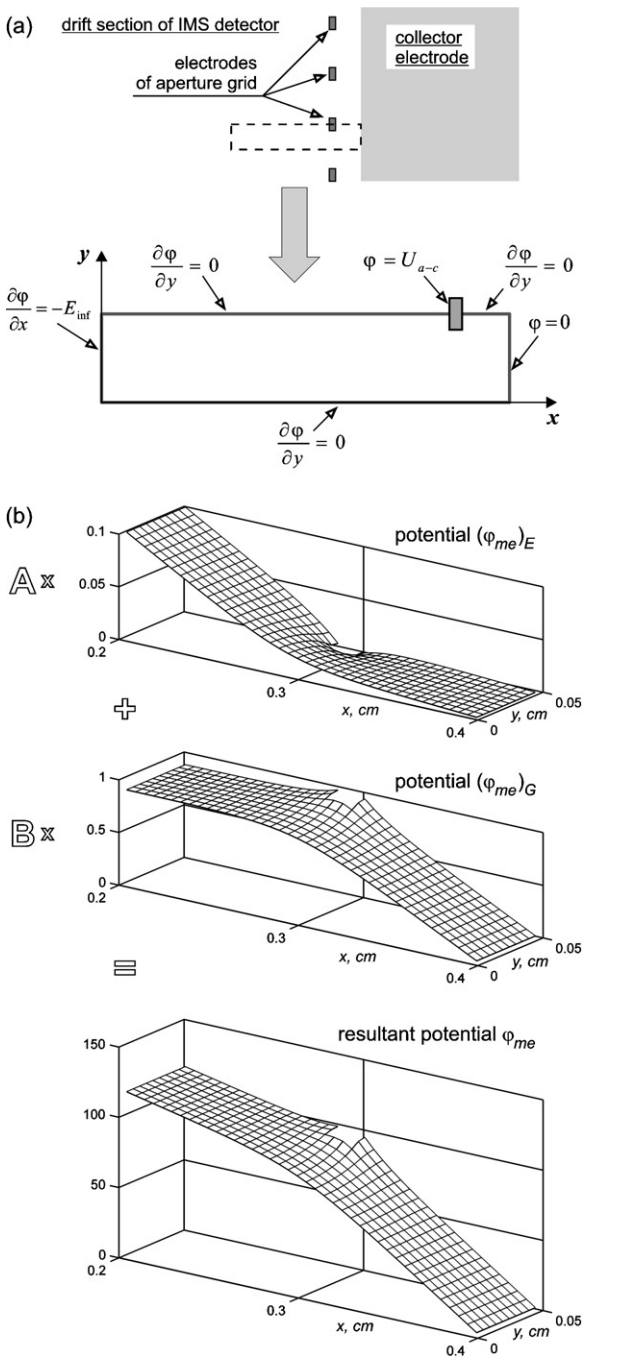

Fig. 2. Method of electric field calculation: (a) geometry and boundary conditions and (b) illustration of superposition rule.

electrodes system, the electric field far from the grid E_{inf}, and difference of potentials between the grid and collector U_{a-c}. In order to avoid the necessity of solving the Laplace equation for each change of the electric field E_{inf} or the grid polarisation voltage U_{a-c} one can take advantage of the fact that the considered problem is linear and the rule of superposition is in force here. The resultant electric potential φ_{me} is a linear combination of potentials generated by the electric field of the drift space and the voltage polarising the aperture grid:

$$\varphi_{me} = \frac{E_{\mathrm{inf}}}{(E_{\mathrm{inf}})_E}(\varphi_{\mathrm{me}})_E + \frac{U_{a-c}}{(U_{a-c})_G}(\varphi_{me})_G \quad (2)$$

where $(\varphi_{me})_E$ and $(\varphi_{me})_G$ are the solutions of the Laplace's equation obtained for special boundary conditions. The potential $(\varphi_{me})_E$ is

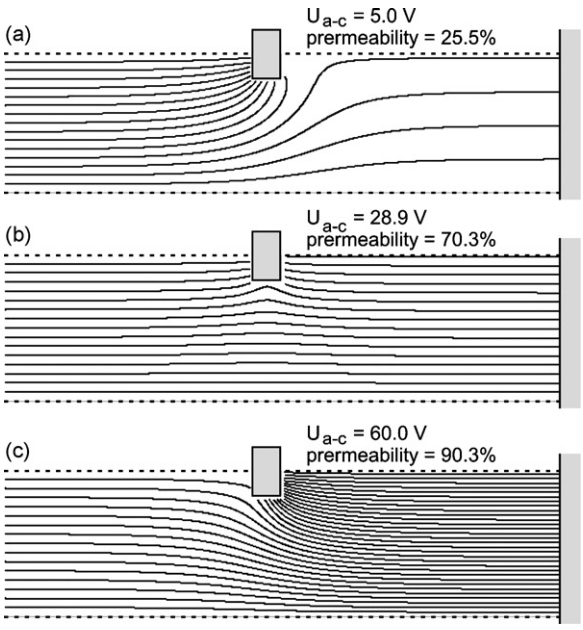

Fig. 3. Electric field lines for three different U_{a-c} voltage values polarizing the grid.

calculated for $E_{inf} = (E_{inf})_E = 1$ V/cm and $U_{a-c} = 0$ V and the potential $(\varphi_{me})_G$ for $E_{inf} = 0$ V/cm and $U_{a-c} = (U_{a-c})_G = 1$ V. The potential distributions $(\varphi_{me})_E$ and $(\varphi_{me})_G$ are characteristic for given geometry and are independent of the potentials of the aperture grid, the collector and the electrodes in the drift section.

The method for calculation of the resultant field based on the rule of superposition is illustrated in Fig. 2b. Three-dimensional graphs of potential distributions enable prediction of ionic movement direction. Positive ions move always along decreasing potential. Shape of the resultant potential indicates that, in the presented case, ions moving towards the collector electrode will bypass the grid electrodes. Analysis of ionic trajectories for flat, two-dimensional geometry can be effectively completed using graphs of the electric field lines. Graphs for the grid constructed of rectangular-cross-section wires are presented in Fig. 3. Electrode dimensions taken for calculations were similar to real size of the aperture grid electrodes in the MedIMS detector, i.e., 0.18 mm × 0.10 mm. The plane passing through centres of electrodes was 1.05 mm away from the surface of the collector electrode. It was assumed that electric field value at appropriate distance from the grid was 275 V/cm.

Three graphs shown in Fig. 3 correspond to different values of the U_{a-c} voltage between the grid and the collector. If the value of that voltage is not too high (Fig. 3a), then most of the electric field lines end on the surface of the grid electrodes. Field lines are good approximation of ion trajectories, therefore it can be concluded that the most of the ions will transfer their charge to the grid electrodes. Increasing the U_{a-c} voltage causes that more and more ions reach the collector. The electric field lines presented in Fig. 3b were drawn for specific case, i.e., for situation when the electric field in the drift section E_{inf} is approximately equal to quotient U_{a-c}/l_{a-c}, where l_{a-c} is a distance between the plane passing through the centres of the grid electrodes and surface of the collector. For a very high difference of potentials between the grid and the collector ionic trajectories bypass the grid electrodes (Fig. 3c).

Analysis of the electric field lines course allows calculation of the grid transmittance, i.e., the ratio of ions flux reaching the collector and ion flux in front of the grid. Relation between transmittance and voltage U_{a-c} is presented in Fig. 4a. Calculations were made for grids placed in a distance of 0.55 and 1.05 mm from the collector. In both cases dimensions of the grid electrodes were the same as for calculation of field lines course. Values of the aperture grid transmittance measured for the MedIMS detector are also presented in Fig. 4a. Measurements were made for an "open" shutter grid. Voltage between the aperture grid and the collector electrode was adjusted using the voltage divider presented in Fig. 1. Quotient of constant current measured in the collector electrode circuit at given U_{a-c} voltage and the current measured at a very high value of that voltage (120 V) was accepted as the experimental value of transmittance. As it is shown, experimental data are close to results of theoretical calculations obtained for the distance l_{a-c} of 1.05 mm.

Measurements of the electric charge carried by the reactant ions in dependence of U_{a-c} voltage were also conducted. During those measurements the shutter grid was working in a normal mode, i.e., it was periodically opened for a short time. Charge of ions was calculated by means of integration of the peak in the drift time spectrum. Obtained results were compared with values of the current measured for open shutter grid (Fig. 4b). The correlation between both quantities, i.e., the charge of ions in the swarm creating the peak and the current being a measure of transmittance, is excellent. Relationships presented in Fig. 4 show that application of relatively high values of U_{a-c} voltage is advantageous from the point of view of signal magnitude.

3.2. Components of the current in collector electrode

Signal of the IMS detector, i.e., a time-dependent current flowing in the collector electrode circuit is a result of two phenomena. The

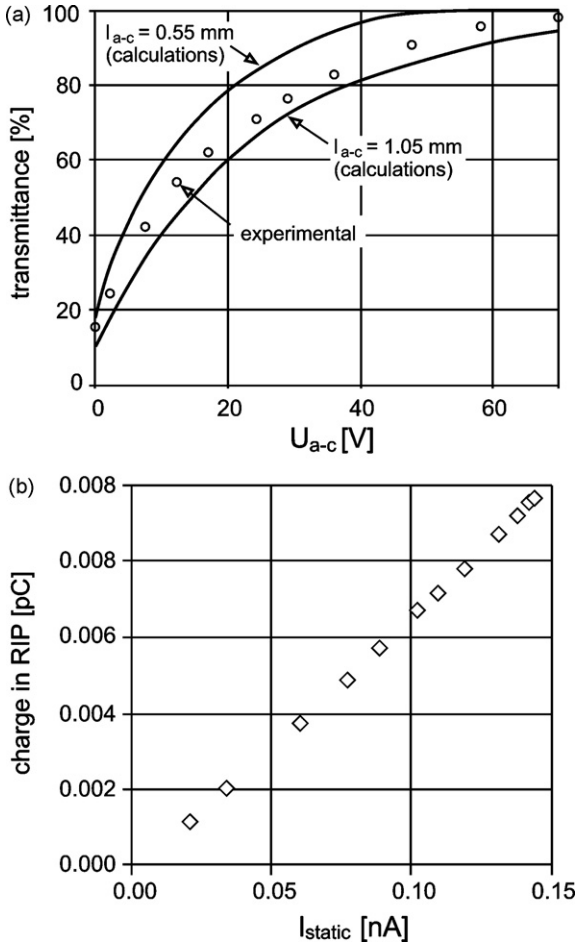

Fig. 4. Calculated and experimental values of the aperture grid transmittance (a) and correlation between current measured for "open" shutter grid and the charge carried by ions creating reactant ions peak (b).

first one is electrical induction caused by ions moving in the drift section and the second one is transfer of ionic charge to the collector electrode. Two components of the collector current i correspond to these two phenomena. They are called induced current i_{ind} and direct current i_{dir}, respectively.

$$i(t) = i_{ind}(t) + i_{dir}(t) \tag{3}$$

Induced current $i_{ind}(t)$ results from the fact that the electric field E_{ion} generated by ion swarm varies in time. According to Gauss' law, the charge density on the surface of the collector is dependent on the value of electric field in the closest vicinity of the surface:

$$\sigma_{ce} = -\varepsilon E_{ce} = -\varepsilon E_{me,ce} - \varepsilon E_{ion,ce} \tag{4}$$

where ε is permittivity constant of gas, in which movement of ions occurs and E_{ce}, $E_{me,ce}$ and $E_{ion,ce}$ are values of electric fields E, E_{me} and E_{ion} on the surface of the collector electrode, respectively. Total electric charge Q_{ce} produced in the collector can be calculated using integrals of the surface charge density over the collector area S_{ce}. Current flowing in the collector circuit is time derivative of total charge. If we define the current flowing out from the collector as a positive one, then the expression for the current induced by ionic movement will have the following form:

$$i_{ind}(t) = -\frac{d}{dt}Q_{ce}(t) = \varepsilon\frac{d}{dt}\int_{S_{ce}} E_{ce}(t)dS_{ce} = \varepsilon\frac{d}{dt}\int_{S_{ce}} E_{ion,ce}(t)dS_{ce} \tag{5}$$

The electric field E_{me} is constant in time, therefore it does affect the induced current value. However, it is necessary to realize that for different values of the E_{me} field, movement of ions in the drift section can be slower or faster. Therefore, time dependence of the ion-generated field varies.

In practice, the charge induced by swarm of ions in the collector appears when those ions are relatively close to the aperture grid and the collector. Initially that charge increases because ion swarm approaches to the collector and the value of E_{ion} field on its surface is growing. Ions reaching the collector and other electrodes become discharged. As a result, the number of ions producing the field E_{ion} decreases and induced charge begins to decrease. Considering movement of positive ions towards the collective electrode, induced current is initially positive and than negative. The characteristic feature of the induced current is that the time integral of this value equals to zero.

Direct current is defined by ion flux reaching a collector. The value of the flux can be calculated on the basis of ionic charge density ρ_{ce} and their velocity v_{ce} in the neighbourhood of the collector surface. If we consider only one kind of ions with mobility coefficient of K, the formula for the direct current has the following form:

$$i_{dir} = \int_{S_{ce}} \rho_{ce}v_{ce}dS_{ce} = K\int_{S_{ce}} \rho_{ce}E_{ce}dS_{ce} \approx K\int_{S_{ce}} \rho_{ce}E_{me,ce}dS_{ce} \tag{6}$$

In typical conditions of IMS detector operation, electric field produced by ions is low compared to the field generated by metal electrodes and for this reason the approximation applied in the formula (6) is justified.

Movement of ions in vicinity of the collector electrode shielded by the aperture grid is illustrated in Fig. 5. When ions are in front of the grid (Fig. 5a), their influence on the collector is low because majority of ion-produced electric field is screened by the grid. Low, increasing current is generated in the collector. After first ions pass through the grid (Fig. 5b), induced current rapidly increases up to the time when ions fill the whole space between the grid and the collector. Then the induced current decreases and direct current starts to flow. In most cases, width of the ionic swarm is greater than the distance from the grid to the collector. During the time in which the space between the grid and the collector is filled by ions (Fig. 5c), induced current is not very high and direct current value results from spatial ion concentration distribution and velocity of ionic movement. In the next phase, number of ions in the space between the grid and the collector quickly decreases. As a result, induced current becomes negative. A schematic course of induced charge, induced and direct current and total current are shown in Fig. 5d.

3.3. Shielding efficiency

Purpose of applying the aperture grid is to limit the region from which ions effectively interact with the collector. An ideal aperture grid should completely eliminate induction of current by ions positioned in front of the grid. In reality, as it is shown in Fig. 5d, ions moving in the drift space generate some small signal. As a result, specific ionic peak is preceded by some relatively slowly growing current. That undesirable signal is lower when shielding of the collector by the grid is more effective. If the total electric charge induced in the collector without the grid is equal Q_0 and introduction of the grid reduces that charge by ΔQ, then quotient of $\Delta Q/Q_0$ can be accepted as a measure of grid shielding properties. That value may be referred to as shielding efficiency. Calculations were carried out in order to determine the relationship between shielding efficiency and width of the grid electrodes as well as the distance between the grid and the collector. It was assumed that the source of electric field is a 0.25-cm-thick layer of space charge of 1.6×10^{-12} C/cm^3 placed in front of the grid. Dimensions and boundary conditions for the space, in which solution of Poisson's equation was sought, are presented in Fig. 6a. The surface charge was calculated from the Gauss's law on the basis of electric field in the vicinity of the collector surface.

If no grid is present in the system we obtain a one-dimensional problem for which the calculation of the electric field is very easy to be accomplished. Value of the electric field on the right side of ionic cloud in Fig. 6a is constant and equal to 4.52 V/cm. Surface charge density σ_{ce0} corresponding to that value of electric field is -0.4 pC/cm^2. Presence of the grid causes non-homogeneity of electric field between the grid and the collector. Therefore, surface charge density depends on y coordinate and for calculation of shielding efficiency an average surface charge density $\sigma_{ce,av}$ should be applied:

$$\text{shielding efficiency} = \frac{\sigma_{ce0} - \sigma_{ce,av}}{\sigma_{ce0}} = 1 - \frac{2}{\sigma_{ce0}d}\int_0^{d/2} \sigma_{ce}(y)dy \tag{7}$$

A relationship between shielding efficiency and width of the grid electrodes h_{ap}, calculated for different distances l_{a-c} between the grid and collector is presented in Fig. 6b.

3.4. The shape of current pulse—theoretical considerations

In order to estimate the shape of current pulse in the collector electrode circuit, time dependencies of induced and direct current have to be calculated. Calculations may be based on Eqs. (5) and (6), but time-dependent distributions of charge density must be determined previously. That task consists in quite complicated solution of advection problem in two-dimensional geometry. Description of a simple numeric method for solution of the problem of the current pulse shape calculation is presented below. The fundamental idea of the method consists in finding the time relationships of the average charge density $\sigma_{ce,av}(t)$ and direct current $i_{dir}(t)$ for specific initial conditions and then using the convolution of functions to obtain the solution for real initial condition given by the charge density distribution in large distance in front of the grid.

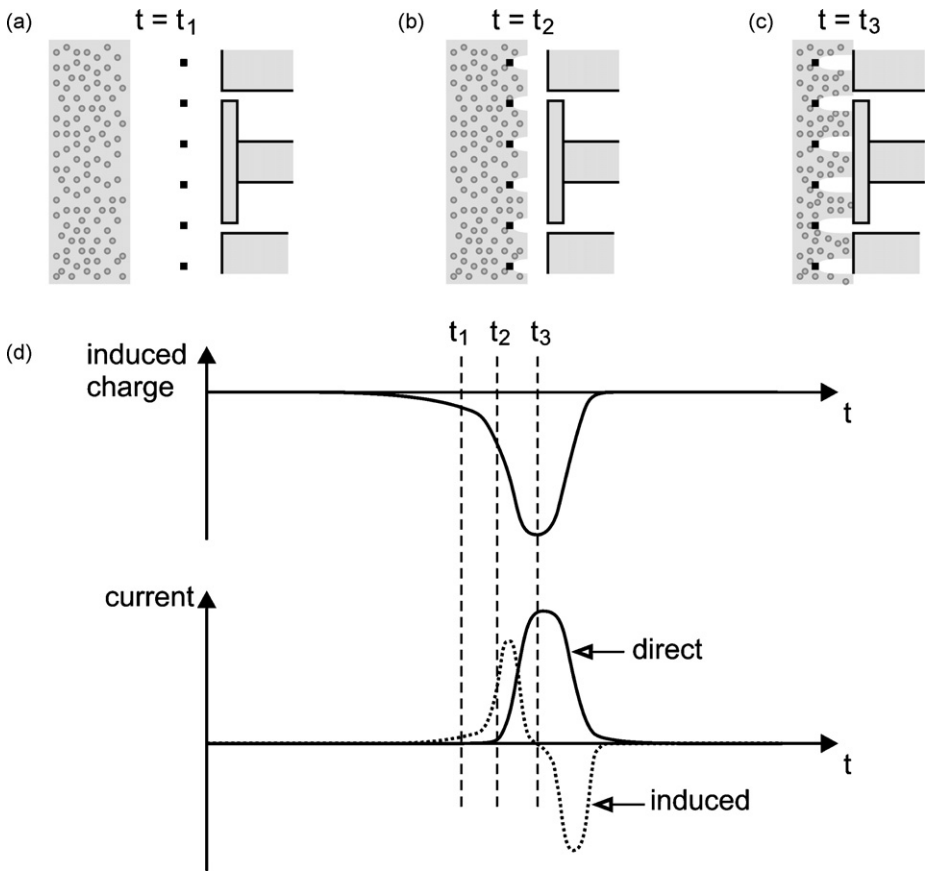

Fig. 5. Mechanism of generation of the collector current components in the IMS detector.

Let us consider a narrow and flat layer of ions with the constant charge density ρ_0 placed at the time $t = 0$ along the plane $x = x_0$ located in large distance in front of the aperture grid (Fig. 7). In successive moments of time the ion cloud moves towards the aperture grid and the collector. The shape of the cloud changes simultaneously. On the final stage of the movement, ions reach electrodes of the aperture grid and the collector. For the time $t = 0$, the layer can by divided into small elements with cross-section of $\Delta x \times \Delta y$. If the electric field and mobility coefficient of ions are known, the position of each element of the layer can be tracked in time. Algorithms for determination of successive positions of elements may be different but in the simplest case for the short time steps Δt_l a relationship between the consecutive positions of i-th element can be expressed by the following formulae:

$$\begin{aligned} x_i(t + \Delta t_l) &= x_i(t) + KE_{me,x}(x_i, y_i)\Delta t_l \\ y_i(t + \Delta t_l) &= y_i(t) + KE_{me,y}(x_i, y_i)\Delta t_l \end{aligned} \tag{8}$$

where $E_{me,x}$ and $E_{me,y}$ are components of the electric field produced by metal electrodes. For successive time steps the electric field and the charge induced on the collector surface by all elements of the layer can be calculated. However, this kind of calculation is complicated and time-consuming because solving the Poisson's equation is necessary for each time step and for each element of layer. In this work another method of calculation of the surface charge was used. It is based on a specifically defined function $s(x,y)$ assigning to each point of space in vicinity of the aperture grid and the collector a special ability to induce an electric charge on the surface of the collector. A brief explanation of the $s(x,y)$ function is given below.

A space charge with the density of $\rho(x,y)$ contained in a small element having dimensions of $\Delta x \times \Delta y$ causes induction of a charge with density of $\Delta\sigma_{ce}(y)$ with average value of $\Delta\sigma_{ce,av}$. The function s is defined as the quotient of average surface charge density and the linear charge which induces that surface charge:

$$s(x, y) \stackrel{def}{=} \lim_{\Delta x, \Delta y \to 0} \frac{\Delta\sigma_{ce,av}}{\rho(x, y)\Delta x \Delta y} \tag{9}$$

Similarly to potentials $(\varphi_{me})_E$ and $(\varphi_{me})_G$ used for calculation of the electric field according to Eq. (2), function $s(x,y)$ depends only on geometry of the system, i.e., it depends on dimensions of grid electrodes, spacing between them and the distance between the grid and the collector. Knowledge of the $s(x,y)$ function for a given system of electrodes is very useful because it facilitates calculation of the average surface charge density for a given distribution of the charge density in the vicinity of the electrode.

$$\sigma_{ce,av}(t) = \int_0^{d/2}\int_0^{x_{ce}} \rho(x, y, t)s(x, y)dxdy \tag{10}$$

Calculations of the $s(x,y)$ function were carried out for the same electrode system as considered in Section 3.1 for determination of the field lines course. Those calculations consisted in multiple (400 times) solution of the Poisson's equation for electric field potential generated by a charge placed in a small volume. For each position of the charge, the value of the electric field on the collector surface was computed and then, based on the Gauss's law, the charge induced on surface was determined. Boundary conditions for the Poisson's equation were as shown in Fig. 6a. Obtained shape of the $s(x,y)$ function is presented in Fig. 8a. It is noticeable that the $s(x,y)$ function is in practice constant in the space in front of the grid, if the distance from the grid is greater than the distance between elec-

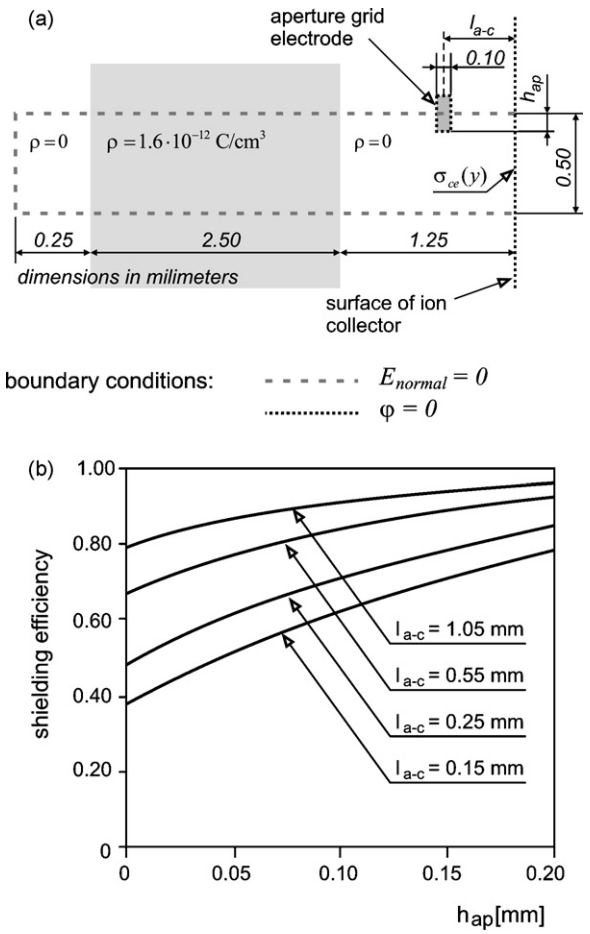

Fig. 6. Geometry assumed for calculation of shielding efficiency (a) and relationship between the collector-grid distance and shielding efficiency (b).

trodes. It is an obvious result of the assumed boundary conditions. Constancy of the $s(x,y)$ function means that independently from the distance from the grid a swarm of ions induces a constant charge in the collector. It is justified for ideally flat geometry, which is a good approximation for small distances between the ionic swarm and the grid. Generally rather strong relationship between the electric field generated by ions near the surface of the collector and a distance should be taken into account. For the MedIMS detector the calculations of the electric field generated by the disc-shaped ionic swarms were carried out. Those calculations showed that when the centre of ionic swarm is placed 0.5 cm from the aperture grid, induced charge is equal to about 14% of the maximum value. For 1.0 cm distance it is only 3%. We found that the relationship between the induced charge and the distance may be approximated by cubic function. Therefore, an appropriate correction of $s(x,y)$ was

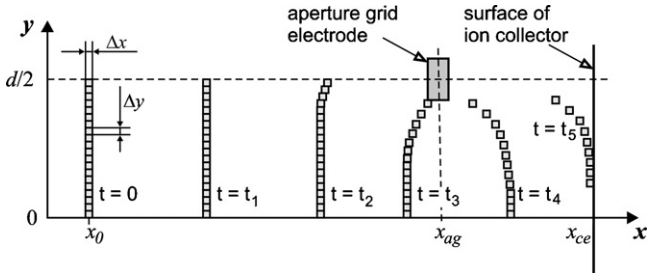

Fig. 7. Movement of ion layer elements in vicinity of the collector electrode—an illustration of the method of peak shape calculation.

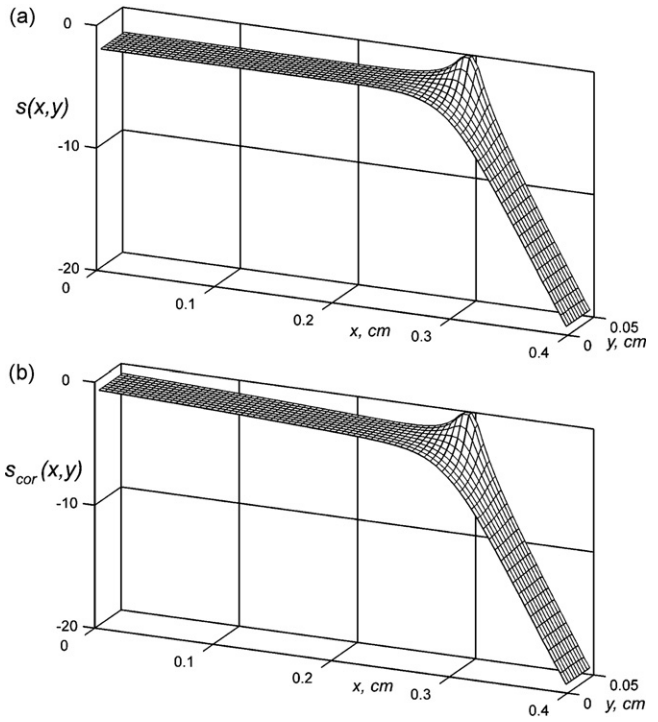

Fig. 8. A function describing a relationship between position of the charge and the average charge induced in the collector electrode. (a) $s(x,y)$ function defined by Eq. (9), (b) values of $s(x,y)$ function after correction given by Eq. (11).

applied:

$$\begin{aligned} s_{cor}(x,y) &= 0 && \text{for } x \le x_0 \\ s_{cor}(x,y) &= \left(\frac{x-x_0}{x_{ag}-x_0}\right)^3 s(x,y) && \text{for } x_0 < x \le x_{ag} \\ s_{cor}(x,y) &= s(x,y) && \text{for } x > x_{ag} \end{aligned} \tag{11}$$

where x_{ag} is a position of the aperture grid, x_0 the smallest value of the x coordinate, for which induction of the charge in the collector electrode should be taken into account. A beginning of the x-axis is located in the middle of the shutter grid. For the MedIMS detector the "constructional" value of x_{ag} is 4.595 cm. The selected value of x_0 is 3.60 cm. The course of the corrected $s(x,y)$ function is shown in Fig. 8b.

Having known the $s(x,y)$ function and positions of particular elements of ionic layer from Fig. 7 it is easy to calculate the time dependence of the average surface charge density induced by all elements of the layer. If the number of elements in the layer is N_l and the width of each element is equal to its height, i.e., $\Delta x = \Delta y = d/(2N_l)$, then the average induced charge density $\sigma^{(1)}_{ce,av}(t)$ can be expressed by the following formula:

$$\sigma^{(1)}_{ce,av}(t) \cong \left(\frac{d}{2N_l}\right)^2 \rho_0 \sum_{i=1}^{N_l} s_{cor}(x_i(t), y_i(t)) \tag{12}$$

Let us assume that the space charge density in the drift section at the moment $t = 0$ depends only on x coordinate and can be described by function $\rho(x,0)$ different from zero only in the range $x_0 - x_{swarm} < x < x_0$, where x_{swarm} is the width of ionic swarm. For the initial condition defined that way, the average density of the charge induced on the collector surface is determined by convolution of the solution for single layer given by the formula (12) and the space

charge density at the moment $t = 0$:

$$\sigma_{ce,av}(t) = \frac{2N_l v}{\rho_0 d} \int_0^{t_{max}} \sigma^{(1)}_{ce,av}(t-\eta)\rho(x_0 - v\eta, 0)d\eta \quad (13)$$

where $v_{drift} = KE_{inf}$ is ion velocity in the drift section and $t_{max} = x_{swarm}/v_{drift}$ is the time during which ions cover the distance equal to the swarm width. Eq. (13) can be written in the form of the sum, convenient for conducting the numerical calculations:

$$\sigma_{ce,av}(t) \cong \frac{2N_l v_{drift}}{\rho_0 d} \Delta t_c \sum_{j=0}^{N_t} \sigma^{(1)}_{ce,av}(t - j\Delta t_c)\rho(x_0 - v_{drift} j\Delta t_c, 0) \quad (14)$$

where $N_t = t_{max}/\Delta t_c$ is the number of time steps and Δt_c is the length of the time step used in calculation of the convolution of functions by numerical integration.

Differentiating of the surface charge density described by Eq. (14) with respect to time gives the average density of the induced current. Total induced current can be obtained from the following formula:

$$i_{ind}(t) = S_{ce} \frac{d\sigma_{ce,av}}{dt} \quad (15)$$

Calculation of direct current is very easy. Tracking the movement of elements of a thin ionic layer from Fig. 7, a number of elements n_k reaching the collector in k-th time step can be estimated. Multiplying that value by the charge contained in the element and dividing by time step duration the value of the direct current $i^{(1)}_{dir}(t)$ generated by the ions contained initially in the narrow flat layer is obtained:

$$i^{(1)}_{dir}(t) \cong S_{ce} \frac{1}{\Delta t_l} \frac{d}{2N_l^2} \rho_0 n_k \quad \text{for} \quad (k-1)\Delta t_l \le t < k\Delta t_l \quad (16)$$

Total direct ion-generated current, for which the initial charge density distribution was described by function $\rho(x,0)$, can be calculated in the way similar to the surface density of the induced charge. The formula analogous to Eq. (14) has the following form for the direct current:

$$i_{dir}(t) \cong \frac{2N_l v}{\rho_0 d} \Delta t_c \sum_{j=0}^{N_t} i^{(1)}_{dir}(t - j\Delta t_c)\rho(x_0 - vj\Delta t_c, 0) \quad (17)$$

3.5. Practical calculations of the peak shape and comparison of results with experimental data

Calculations of relationships between time and the charge induced in the collector and the direct current were carried out with the IMS-AG program. Input data used for further calculations were matrixes containing the values of functions $(\varphi_{me})_E$, $(\varphi_{me})_G$ and s_{cor}. They are characteristic for given dimensions of electrodes shaping the electric field in the vicinity of the collector. Those data were calculated with the MATLAB software. User-changed parameters in the IMS-AG program are: the mobility coefficient K, value of the electric field in great distance from the aperture grid E_{inf}, potential difference between the grid and the collector U_{a-c}, duration of time step Δt_l and gating time of the shutter grid t_g. It was assumed that the space charge density $\rho(x,0)$ in the ionic cloud in front of the aperture grid can be described by difference of error functions. The equation, according to which calculations were carried out, was obtained after suitable transformations of the well-known formula brought out by Spangler and Collins [7]:

$$\rho(x,0) = \frac{\rho_0}{2}\left[erf\left(\frac{x - x_1}{\Delta x_{dyf}}\right) - erf\left(\frac{x - x_2}{\Delta x_{dyf}}\right)\right] \quad (18)$$

where $x_1 = x_0 - 2\Delta x_{dyf} - v_{drift} t_g$, $x_2 = x_0 - 2\Delta x_{dyf}$, $\Delta x_{dyf} = 2\sqrt{D_L t_0}$ are the width of the edge of distribution, D_L the longitudinal diffusion coefficient, $t_0 = x_0/v_{drift}$ the time of ions' drift from shutter grid to position $x = x_0$, ρ_0 are the space charge density directly after the injection of ions into the drift section.

Value of the diffusion coefficient D_L was estimated from the Einstein's formula based on ion mobility coefficient. All calculations were made for the space charge density ρ_0 of 1.6×10^{-12} C/cm^3. It is easy to show that the charge density described by Eq. (18) is practically different from zero only in the range $x_0 - x_{swarm} < x < x_0$, for the width of the swarm of $x_{swarm} = 4\Delta x_{dyf} + v_{drift} t_g$.

Successive positions of the layer elements were calculated based on Eq. (8). The surface charge of the collector and the direct current generated by moving ions from the narrow layer were calculated from Eqs. (12) and (16). Eqs. (14) and (17) were used for calculation of the total charge and the direct current. Those results constitute output data from the IMS-AG program and may be saved in text files.

Time dependencies of the induced charge and components of the current are presented in Fig. 9. Those graphs were prepared for two values (5 or 40 V) of voltage U_{a-c} between the grid and the

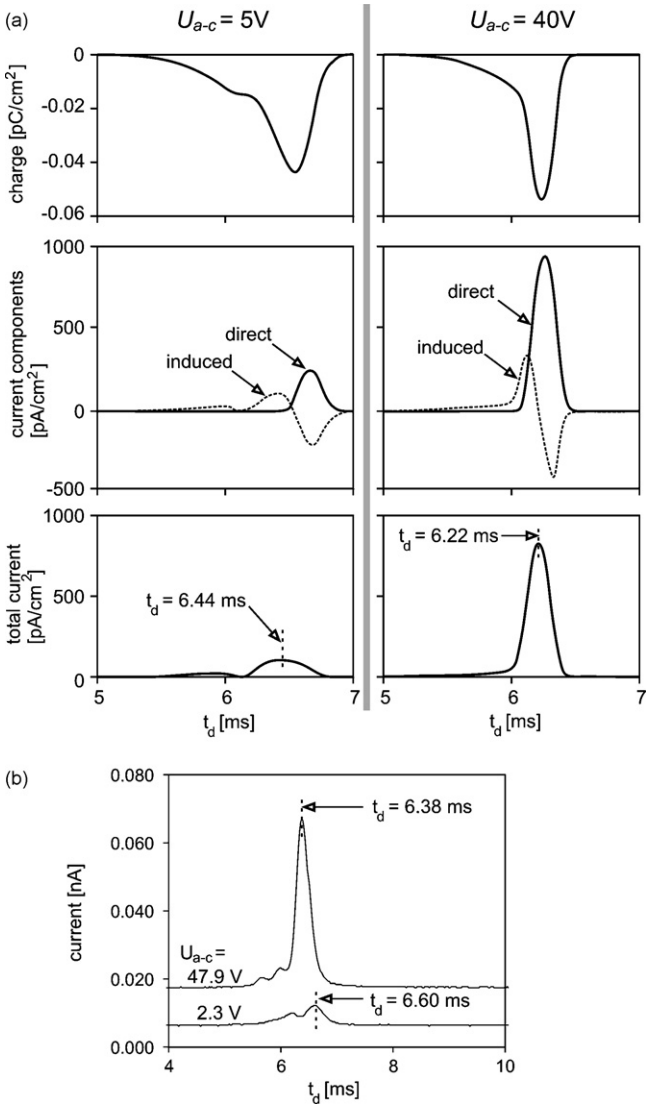

Fig. 9. Induced charge, current components and total current for lowered (5 V) and normal (40 V) voltage between the aperture grid and the collector (a). Experimental results of collector current measurements (b).

collector. The higher value of voltage corresponds to normal polarisation of the grid, guarantying appropriately high transmittance (about 80%). Pulses of the induced and direct currents have high amplitude and are relatively short. For U_{a-c} voltage equals to 5 V amplitude of the induced current is lower because changes of the surface charge occur more slowly. Amplitude of the direct current is also lower, which is caused by low grid transmittance (26%). An interesting phenomenon occurring for small voltages polarising the grid is presence of two peaks in the drift time spectra. Explanation of that effect is relatively simple. For high values of U_{a-c} voltage, the drop of the induced current resulting from filling of the space between the grid and the collector by ions is compensated by fast increasing direct current, which is generated by almost all the ions. If the U_{a-c} voltage is low, then the direct current does not compensate the drop of induced current because most of the ion charge is transferred to the grid electrodes.

Drift time spectra of reactant ions in the air measured with the MedIMS spectrometer for two different values of U_{a-c} voltage are presented in Fig. 9b. It is noticeable by analysing graphs a and b that the proposed theoretical model allows prediction of basic effects evident from measurements. As U_{a-c} voltage increases the amplitude and the area of the peak increase as well. That effect is obviously associated with the relationship between transmittance and U_{a-c} voltage. Another phenomenon is shifting the peak maximum towards the shorter drift times with increasing U_{a-c} voltage. It is evident from both theoretical and experimental data.

The exact comparison of peak shapes obtained from measurements and calculations is impossible because calculations were made for arbitrarily assumed distribution of space charge in a swarm in front of the grid. Furthermore, modeling was carried out for one kind of ions only, while there are three ionic species (ammonium, $NO^+(H_2O)_n$ and hydronium) in the experimental drift time spectra. However, theoretical calculations allow predicting two characteristic peak shape-related effects. Firstly, presence of two maxima in the drift time spectra, shown in Fig. 9a as a result of calculations for small values of U_{a-c} voltage is experimentally verifiable. That is clearly visible in Fig. 9b for $U_{a-c} = 2.3$ V and also can be found in experimental data from the literature [17]. The second qualitative effect associated with generation of current in the collector electrode is a slow increase of the current preceding a characteristic peak. That effect can be observed in results of calculations as well as in the experimental data. For both kinds of results intensity of the current preceding the peak is independent on the U_{a-c} voltage.

4. Conclusions

Phenomena occurring in the system of the aperture grid and the collector electrode in the IMS detectors significantly influence magnitude and shape of peaks in drift time spectra. The model of processes related to generation of signal in the collector electrode presented in this paper allows correct prediction of current pulse shapes and estimation of signal parameters.

Development of a model of such accuracy required consideration of two mechanisms of the collector current generation, i.e., electrostatic induction and collection of ions. Those phenomena had to be described for aperture grid of determined structure with electrodes of defined shape and dimensions, located in a defined distance from the collector. It was necessary to solve mathematical problems in two-dimensional geometry. That approach gave proper explanation of amplitude and the peak area relationships with voltage between the grid and the collector. Determination of shielding efficiency for different dimensions of the grid electrodes was also possible.

Of course, every mathematical model is only an approximation of a real system. Complex three-dimensional models can also be created for the ion collector and the aperture grid in the IMS detector. Models of that kind may be justified for shapes of metal electrodes in the drift section. Usually those electrodes have form of rings with axis of symmetry perpendicular to the grid electrodes. Calculations carried out for three-dimensional geometry are much more complicated and analysis of obtained results is more difficult. In the present study we have avoided those problems using suitable correction for calculation of the charge induced in the collector by ions moving deep in the drift section. Therefore it was possible to determine shape of the initial part of current pulse.

Effect of aperture grid and collector electrode structure on peak width, i.e., on the resolving power, was not studied. It is possible to perform such investigations by “computer experiments” with use of IMS-AG program. Results obtained that way could be applied for optimisation of construction of IMS detectors.

Acknowledgements

This work has been supported by a Marie Curie Transfer of Knowledge Fellowship of the European Community’s Sixth Framework program under contract number MTKD-CT-2006-042637. BS acknowledges the financial support from the project PBS770/MUT.

References

[1] M.J. Cohen, F.W. Karasek, J. Chromatogr. Sci. 8 (1970) 330–337.
[2] T. Tuovinen, H. Paakkanen, O. Hänninen, Anal. Chim. Acta 440 (2001) 151–159.
[3] I.A. Buryakov, E.V. Krylov, E.G. Nazarov, U.Kh. Rasulev, Int. J. Mass Spectrom. Ion Proc. 128 (1993) 143–148.
[4] B.M. Kolakowski, Z. Mester, Analyst 132 (2007) 842–864.
[5] G.R. Asbury, H.H. Hill Jr., J. Microcolumn Sep. 12 (2000) 172–178.
[6] I.W. Leonhardt, W. Rohrbeck, H. Bensch, Int. J. Ion Mobility Spectrom. 3 (2000) 43–49.
[7] G.E. Spangler, C.I. Collins, Anal. Chem. 47 (1975) 403–407.
[8] G.E. Spangler, Anal. Chem. 64 (1992) 1312.
[9] J. Xu, W.B. Whitten, J.M. Ramsey, Anal. Chem. 72 (2000) 5787–5791.
[10] M. Salleras, A. Kalms, A. Krenkow, M. Kessler, J. Goebel, G. Muelle, S. Marco, Sens. Actuators B: Chem. 118 (2006) 338–342.
[11] J. Puton, A. Knap, B. Siodłowski, Sens. Actuators B: Chem. 135 (2008) 116–121.
[12] W.F. Siems, C. Wu, E.E. Tarver, H.H. Hill Jr., P.R. Larsen, D.G. McMinn, Anal. Chem. 66 (1994) 4195–4201.
[13] Ch. Wu, W.E. Steiner, P.S. Tornatore, L.M. Matz, W.F. Siems, D.A. Atkinson, H.H. Hill Jr., Talanta 57 (2002) 123–134.
[14] G.E. Spangler, Int. J. Mass Spectrom. 220 (2002) 399–418.
[15] A. Kalms, M. Salleras, Z. Liu, J.G. Korvink, J. Goebel, G. Muller, J. Samitier, S. Marco, Numerical simulation of ion drift within ion mobility spectrometers in high Peclet conditions using FEM techniques, in: Proceedings of International Conference on Thermal, Mechanical and Multi-Physics Simulation Experiments in Microelectronics and Micro-Systems, EuroSime 2007, London, UK, 16–18 April, 2007, pp. 1–6.
[16] http://www.mathworks.com/products/matlab/.
[17] G.A. Eiceman, E.G. Nazarov, J.E. Rodriguez, J.A. Stone, Rev. Sci. Instrum. 72 (2001) 3610–3621.